HUNGARIAN JOURNAL OF
INDUSTRY AND CHEMISTRY
Vol. 53(2) pp. 7–16 (2025)
hjic.mk.uni-pannon.hu
DOI: 10.33927/hjic-2025-12

POTASSIUM HYDROXIDE-ACTIVATED PALM KERNEL SHELL CARBON FOR METHYLENE BLUE ADSORPTION: REAGENT RECOVERY AND REGENERATION STRATEGIES

TEOW ZI XIAN[1], FADINA AMRAN[2], AGUS ARSAD[1] AND MUHAMMAD ABBAS AHMAD ZAINI[1-2]*

1 Faculty of Chemical & Energy Engineering, Universiti Teknologi Malaysia, 81310 UTM Johor Bahru, Johor, MALAYSIA
2 Centre of Lipids Engineering and Applied Research (CLEAR), Ibnu Sina Institute for Scientific and Industrial Research, Universiti Teknologi Malaysia, 81310 UTM Johor Bahru, Johor, MALAYSIA

This study investigates the preparation and characterization of activated carbon derived from palm kernel shell, utilizing recovered potassium hydroxide (KOH) as the activating agent. The research seeks to address dye water pollution and the release of toxic chemicals from washing activated carbon upon its activation that are detrimental to aquatic ecosystems. Fresh activation was performed in a furnace at a temperature of 550 °C for one hour. The resultant activated carbon was washed and the recovered KOH solution was used for subsequent activation. The activated carbons were characterized to determine their surface area, morphology, functional groups and batch adsorption capacity. The fresh activated carbon exhibited a yield of 14.2% and a surface area of 7.24 m²/g. Notably, the surface area of 55.1 m²/g of the activated carbon produced using recycled KOH solution was greater with an enhanced level of methylene blue removal. The adsorption data could be described by the Redlich-Peterson isotherm and pseudo-second-order kinetic models, suggesting a hybrid of physicochemical interactions. The adsorption process is endothermic and spontaneous when the temperature of the solution is high. This work also showcases the regeneration of activated carbon by using 0.1 M HCl and distilled water as solvents, underscoring the sustainability and cost-effectiveness of manufacturing activated carbon.

Keywords: adsorption, activated carbon, methylene blue, palm kernel shell, potassium hydroxide, reagent recovery

1. Introduction

The rapid increase in the global population has led to a significant rise in pollution levels across various environments. Among the most considerable problems the world is experiencing currently is water pollution, moreover, one of the major contributing factors is the industrial discharge of dyes. Reports state that roughly 10 to 20% of dye molecules are released into the environment along with industrial wastewater, triggering detrimental effects to aquatic life and human health [1]. According to the Environmental Quality Report for Malaysia, dye waste produced in the textile industry in Malaysia has escalated to nearly 800 tons and accounts for 22% of wastewater produced in the country [2]. Several treatments have been introduced to address the issue of wastewater pollution, moreover, one of the preferred and effective methods is activated carbon adsorption. Activated carbon is a porous carbon-based adsorbent with a large surface area, allowing it to adsorb a wide range of pollutants from water.

Commercially available activated carbon derived from coal and petroleum pitch is renowned for its outstanding adsorption performance, making it an excellent choice for environmental protection. However, its high cost somewhat inhibits broad applications across various industries [3]. Malaysia is well known for its abundance of palm oil. Nearly 4.3 million tons of palm kernel shell (PKS) are generated yearly [4], making it an abundant and underutilized biomass resource in the palm oil industry. PKS is a potent carbon feedstock for manufacturing activated carbon as well as provides a sustainable and eco-friendly approach to wastewater treatment.

Activated carbon is produced through a process known as activation. Potassium hydroxide (KOH) is among the most common used activators to develop a porous network within a carbon matrix. Nonetheless, the reagent is toxic and could result in secondary pollution due to its release during the washing of activated carbon. Therefore, the washed water from the aforementioned step must be cautiously handled to minimize undesirable impacts to human health and the environment [5].

Received: 1 Apr 2025; Revised: 20 Apr 2025;
Accepted: 30 Apr 2025
*Correspondence: abbas@cheme.utm.my

Conventional washing can be employed as a reagent recovery method to minimize the release of spent KOH. Distilled water was used to dissolve, extract and recover spent KOH from the activated carbon. The washing liquid was collected and reused for subsequent activation [4] in order to manufacture another batch of activated carbon, while minimizing the chemical discharge. This supports the circular economy initiative within the activated carbon industry.

In this work, methylene blue adsorption was performed to evaluate the performance of PKS activated carbons. The equilibrium, kinetics and thermodynamics of dye adsorption were analyzed as well as discussed to provide an insight into the governing mechanisms. Since dealing with dye-loaded activated carbon remains challenging, identifying suitable solvents for regeneration is also crucial for resource recovery [6].

2. Experimental

Palm kernel shell was collected from Felda Taib Andak palm oil mill. The model dye, methylene blue (MB, $C_{16}H_{18}ClN_3S$, 319.85 g/mol) was purchased from R&M Marketing, UK. All chemicals used are analytical-grade reagents.

2.1. Preparation and characterization of activated carbon

Potassium hydroxide (KOH) was dissolved and mixed with 20 g PKS in a KOH:PKS weight ratio of 2:1. The mixture was impregnated in an oven at 110 °C overnight. The dried sample was activated in a furnace at 550 °C for 1 h and the resultant activated carbon denoted as AC1. Next, it was washed using distilled water to recover the excess KOH and the wash water was used for another activation with 20 g of PKS. The previous steps were repeated and the resultant activated carbons were designated as AC2 and AC3. For the purpose of a comparison, PKS char was produced without KOH at 550 °C for 1 h.

The textural properties of the activated carbon samples were determined using a surface area analyzer by following the Brunauer-Emmett-Teller (BET) method. The surface morphology of the sample of activated carbon was obtained by a TM3000 tabletop scanning electron microscope (Hitachi, Japan). The surface functional groups were qualitatively identified from peak assignments using a Spectrum One Fourier transform infrared spectrometer [4].

2.2. Adsorption studies

MB solutions of various concentrations ranging from 25 to 200 mg/L were prepared by diluting the stock solution. The flasks containing 20 mL of solution were loaded with 20 mg of activated carbon and the mixtures allowed to equilibrate at room temperature for 72 h. Next, the residual concentrations were measured using a SpectrumLab 752 Pro UV-Vis spectrophotometer at a wavelength of 620 nm. The dye capacity at equilibrium, q_e, was calculated according to the method applied in previous studies [7],[8]:

$$q_e = \frac{(C_o - C_e)}{W} V \quad (1),$$

where C_o and C_e (mg/L) denote the initial and equilibrium concentrations, respectively, V (L) stands for the volume of the solution while W (g) represents the mass of activated carbon.

The effect of the contact time was analyzed by measuring the residual concentrations of dye solution at preset intervals from the 5 mins after the activated carbon was loaded into the solution until equilibrium was attained. Multiple dye concentrations were prepared to demonstrate the change in capacity over time until equilibrium was reached. Adsorption at time t, q_t, was calculated as [8]:

$$q_t = \frac{(C_o - C_t)}{W} V \quad (2),$$

where C_t (mg/L) denotes the dye concentration at a specified time.

The effect of temperature on dye adsorption was investigated for AC1 at solution temperatures of 30, 45 and 55 °C. The temperature was adjusted using a temperature-controlled water bath. The dye concentration was fixed at 50 mg/L and the mixtures were left for 72 h.

2.3. Regeneration studies

Distilled water and 0.1 M HCl were prepared as solvents to regenerate spent activated carbon AC1. 20 mg MB-loaded AC1 was mixed with 20 mL of solvent at room temperature for 72 h [6]. The desorption capacity, q_d, was calculated as:

$$q_d = \frac{C_f V}{W} \quad (3),$$

where C_f (mg/L) denotes the dye concentration in the desorbing solution. The desorption efficiency, $D\%$, was calculated as:

$$D\% = \frac{q_d}{q_e} \times 100 \quad (4).$$

The regeneration efficiency, $R\%$, was calculated as:

$$R\% = \frac{q_f}{q_i} \times 100 \quad (5),$$

where q_f denotes the MB adsorption capacity after regeneration and q_i represents the adsorption capacity using fresh AC1. The adsorption and desorption experiments were repeated over 4 cycles.

3. Results and discussion

3.1. Characteristics of activated carbon

The textural properties of AC1, AC2 and AC3 are summarized in *Table 1*. The pH of all ACs was basic from 8.9-9.6 due to chemical reactions during activation.

Table 1: Textural properties of AC1, AC2 and AC3

Sample	AC1	AC2	AC3
pH	9.6	8.9	9.4
Yield (%)	14.2	30.3	29.9
BET surface area (m^2/g)	7.24	30.3	55.1
Total pore volume (cm^3/g)	0.0211	0.0196	0.0298
Micropore volume (cm^3/g)	0.00131	0.00811	0.0174
Mesopore volume (cm^3/g)	0.0198	0.0115	0.0124
Average pore size (nm)	11.7	2.59	2.16

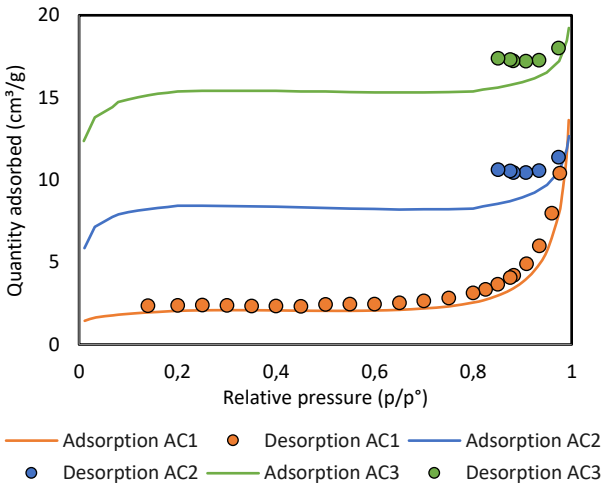

Figure 1: N_2 adsorption-desorption isotherms of AC1, AC2 and AC3

The KOH activator interacts with the carbon matrix, thereby producing several potassium species. Potassium ions (K^+) in particular are known for their basic nature in activated carbon [9].

The yield of activated carbon ranked as AC2 ≈ AC3 > AC1. AC1 recorded the lowest yield of 14.2 %, while AC2 and AC3 yielded 30 %. The lower yield of AC1 was due to aggressive carbon burning-off and the dehydrating effect of KOH during carbonization. The heating process is anticipated to encourage bond cleavage of weakly connected bridges in the impregnated material, releasing volatiles and causing subsequent weight loss caused by oxidation reactions [3]. In contrast, the greater yield observed for AC2 and AC3 may have resulted from the less significant dehydrating effect of KOH. The amount of KOH recovered upon activation is presumably less as some has been consumed and evaporated during the initial activation.

The BET surface area of the ACs ranked as follows: AC3 (55.1 m^2/g) > AC2 (30.3 m^2/g) > AC1 (7.24 m^2/g). Generally, the higher KOH ratio leads to an increase in the surface area of activated carbon. The KOH enhances the development of pores during the carbonization process. Nevertheless, an optimal ratio is found beyond which a further increase in the amount of KOH decreases the surface area. An excessive amount of KOH used in activation significantly damages the carbon structure, collapsing the pore walls and producing larger pores at the expense of smaller ones [10]. This relationship is illustrated by the average pore size of ACs as presented in *Table 1* in the order of AC1 > AC2 > AC3.

The N_2 adsorption-desorption isotherms of AC1, AC2 and AC3 are depicted in *Figure 1*. All ACs exhibit characteristics of Type IV isotherms typically associated with mesoporous materials (pore sizes ranging from 2 to 50 nm). A key feature of this isotherm is the presence of hysteresis loops, which arise from capillary condensation within the pores, indicating that the adsorption and desorption processes do not follow the same mechanism. The observed hysteresis loop for AC1 suggests significant capillary condensation within its pores. In contrast, the shape of the hysteresis loops for AC2 and AC3 implies a unique pore texture, resembling that of ink-bottle or slit-like pores.

The pore size distribution of the ACs is displayed in *Figure 2*. The curves typically exhibit distinct peaks corresponding to specific pore widths, highlighting where most of the surface area is concentrated. For AC1, a sharp peak at 2 nm suggests the predominance of micropores (pore width < 2 nm) and small mesopores (~2 - 3 nm), while a small but consistent increase in pore volume thereafter for pore widths ranging from 5 to 15 nm indicates the contribution of mesopores. Conversely, AC2 and AC3 only demonstrate a peak centered at 2 nm, suggesting that they are highly microporous with a minimal amount of mesopores.

The presence of functional groups such as O–H, C=C, C–O, C–H, C–H and C≡C plays a considerable role in MB adsorption. The hydroxyl (O–H) groups form hydrogen bonds with dye molecules and act as acidic sites to facilitate ion exchange [7],[11]. The carbonyl (C=O) groups are electrostatically attracted to positively charged dye molecules, moreover, can form complexes with MB, thereby increasing the removal performance [12]. The ether and ester (C–O) linkages enhance the reactivity of the carbon surface, increasing the likelihood of interactions with dye molecules [12]. Furthermore, the presence of C–H bonds promotes hydrophobic interactions with non-polar moieties of MB [12]. Additionally, alkynes (C≡C) and a graphitic surface facilitate non-covalent interactions via π-π stacking between the aromatic rings of methylene blue [7],[13].

As shown in *Figure 3*, all the activated carbons exhibit identical spectral patterns. Notably, the intensity of some peaks for AC1 is greater than for AC3. The abundance of acidic oxygen functional groups like hydroxyl (O–H) in AC1 suggests a stronger affinity to interact with MB. Furthermore, AC1 contains more aromatic C=C groups than AC3. This observation is in line with the adsorption performance, wherein AC1 outperforms AC3 although the surface area of the former is smaller.

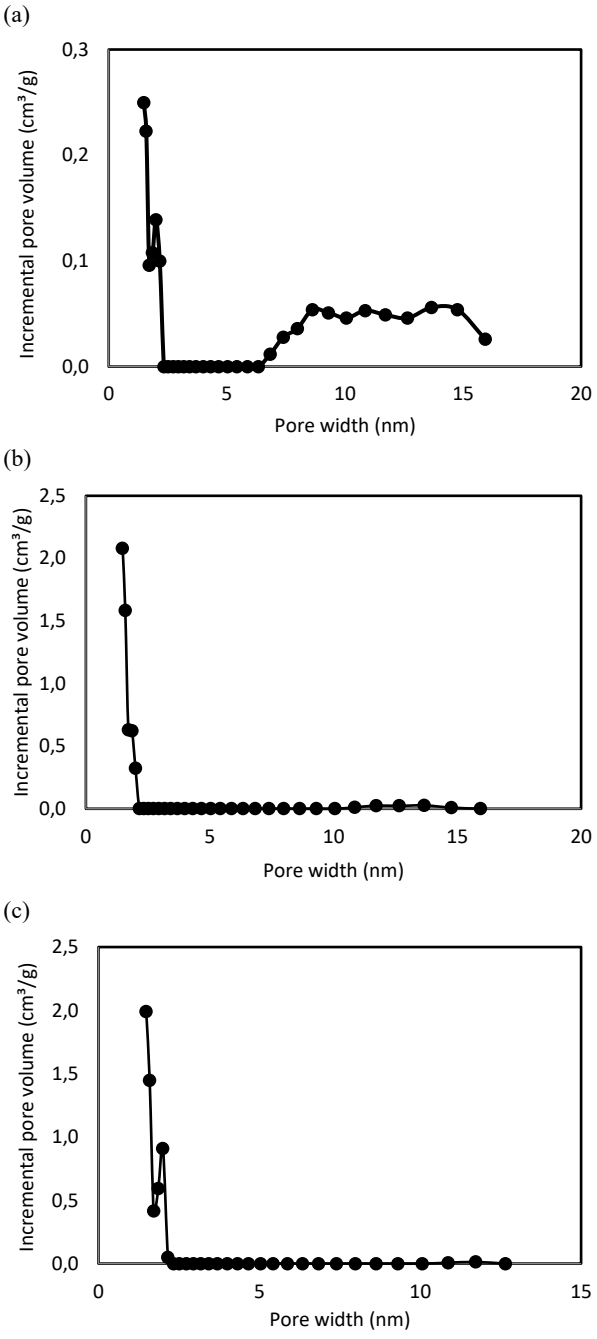

Figure 2: Incremental pore volume vs. pore width of (a) AC1, (b) AC2 and (c) AC3

The surface morphology of the ACs is shown in *Figure 4*. AC2 and AC3 exhibit a well-developed porous texture characterized by a honeycomb-like structure. In contrast, AC1 displays a surface with rudimentary pores that correlates well with its lower surface area and possible pore collapse during activation.

3.2. Equilibrium adsorption

An adsorption isotherm describes the equilibrium between the amount of dye adsorbed and its concentration in the solution [14]. The equilibrium of MB adsorption onto KOH-activated carbons is shown in *Figure 5*. Generally, the dye capacity increases as the

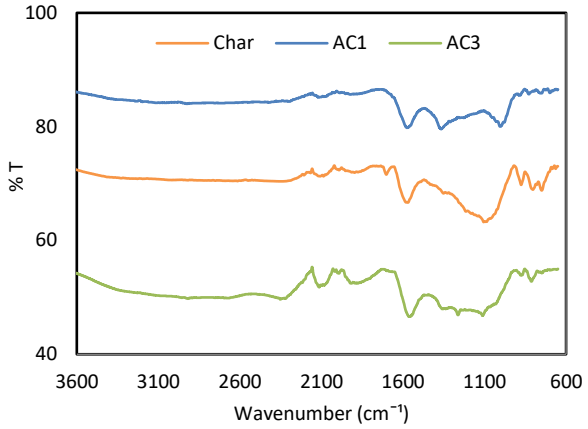

Figure 3: FTIR spectra of char, AC1 and AC3

concentration increases. The concentration gradient acts as a driving force to enhance the transport of dye molecules to overcome the mass transfer resistance between the aqueous (bulk) and solid phases [3]. Dye molecules can be lodged into surfaces with vacant sites prior to reaching its saturation limit that determines its maximum capacity.

The level of adsorption (q_e) increases as the concentration (C_e) increases in all curves but levels off as different removal capacities are reached. The concave upward shape implies preferable dye removal onto AC samples [15]. The adsorption capacity is proportional to the concentration until the sites become mostly occupied at higher concentrations. At this point, the level of affinity subsides and q_e increases at a diminishing rate [16].

The adsorption of MB follows the order given: AC1 > AC3 > AC2 > Char. This infers the importance of KOH activation in developing the surface chemistry and texture of AC samples for MB adsorption. AC1 exhibits a higher dye capacity of 35 mg/g. The superior performance of ACs is partly attributed to its higher pH that encourages the deprotonation of oxygenated groups such as carboxyl, phenolic and hydroxyl. The hydroxide ions (OH^-) in the solution facilitate the removal of protons from these acidic groups, thereby creating the negatively charged sites on the carbon surface which are electrostatically attracted to the cationic dye molecules. The optimal pH for MB adsorption typically falls between pH 7 and 11, combining the effects of increased negative charge on the carbon surface and reduced competition with protons (H^+) [17]. A greater removal rate by AC3 when compared to AC2 also signifies the roles of basic solutions and deprotonation on MB adsorption.

In conclusion, the oxygen-containing functional groups release protons, rendering the carbon surface negatively charged [18]. Methylene blue is a basic dye that carries a positive charge [19] and will adhere onto the surface via electrostatic attraction, coordination mechanisms and the formation of complexes. The driving force for adsorption is essentially powered by the concentration difference between the bulk solution

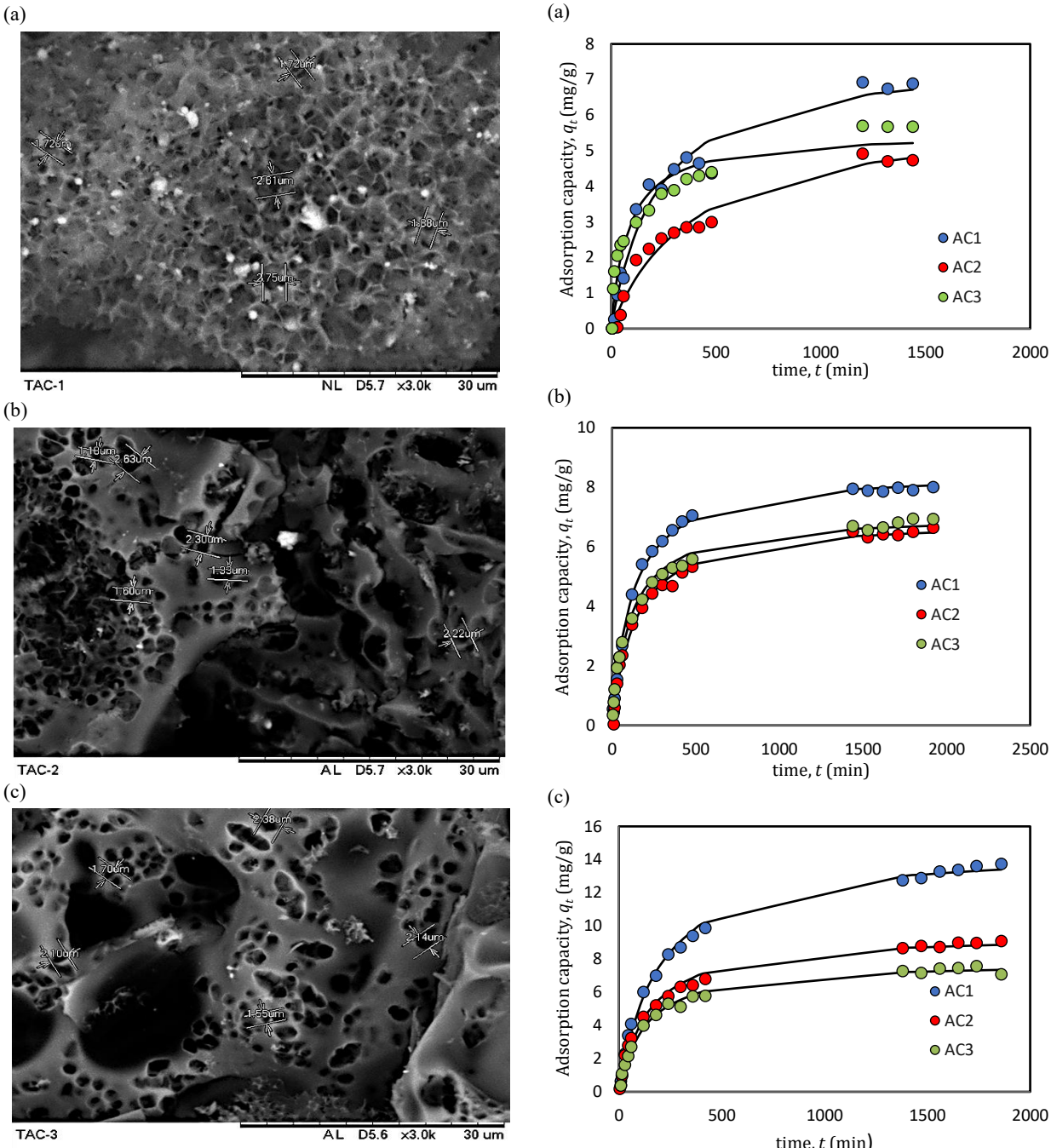

Figure 4: SEM images of (a) AC1, (b) AC2 and (c) AC3 at a magnification of 3000×

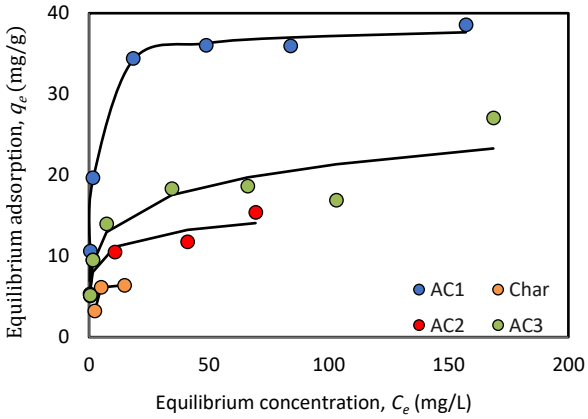

Figure 5: Equilibrium of MB removal onto KOH-activated carbons

Figure 6: Rate of methylene blue adsorption by activated carbons at concentrations of (a) 5.0, (b) 8.5, (c) 14.5 and (d) 25.0 mg/L

Table 2: The constants of isotherm models for methylene blue adsorption by KOH-activated carbons

Sample	Char	AC1	AC2	AC3
Langmuir				
Q_m (mg/g)	7.90	37.5	13.2	20.7
b (L/mg)	0.399	0.696	1.22	0.450
SSE	1.32	5.83	10.7	65.3
R^2	0.795	0.995	0.809	0.787
Freundlich				
K_f	3.20	15.3	7.10	8.04
n	3.60	4.96	5.97	4.72
SSE	2.16	133	8.26	39.7
R^2	0.654	0.886	0.853	0.867
Redlich-Peterson				
A	1.36	27.5	37.3	40.8
B	0.00120	0.785	4.25	4.23
G	2.77	0.984	0.887	0.827
SSE	0.00	5.14	7.21	37.3
R^2	1.00	0.996	0.872	0.875

and carbon surface [20]. However, the driving force diminishes over time as an equilibrium is reached. AC1 exhibits a greater affinity that indicates a strong tendency to bind with dye molecules at low dye concentrations [14]. Typically, this is due to high-energy adsorption sites that are composed of carboxyl, phenolic and hydroxyl groups [21].

Three isotherm models, namely Langmuir, Freundlich and Redlich-Peterson, were used to analyze as well as describe the equilibrium data of dye adsorption. The constants of isotherm models are presented in *Table 2*, calculated using Solver add-in in Microsoft Excel by minimizing the sum of squared errors (SSE) to achieve the best correlation coefficient (R^2). All carbon samples fell in line with the Redlich-Peterson isotherm with $R^2 > 0.88$. The applicability of this model suggests a monolayer coverage on homogeneous and heterogeneous surfaces, thereby giving rise to a hybrid of physicochemical adsorption mechanisms [22].

3.3. Adsorption kinetics

The contact time between the dye molecules and activated carbon determines the degree of adsorption and provides insights into the adsorption kinetics [14]. The rate of MB adsorption onto AC samples at different concentrations is shown in *Figure 6*. The dye capacity increases with the holding time, confirming a time-dependent process [14]. Rapid adsorption during the first 300 mins is ascribed to the plentiful availability of active sites for MB removal. The adsorption rate started to reduce because of repulsion between dye molecules once sites became occupied. It was observed that longer contact times would be required at higher dye concentrations. The contact time for adsorption to reach equilibrium at low concentrations of 5.0-8.5 mg/L is approximately 200-600 mins, while 800-1400 mins is needed at concentrations of 14.5-25.0 mg/L. Initially, dye molecules have to overcome the boundary layer effect before diffusing into the surface of activated carbon then further diffusing into the porous network of activated carbon and finally interacting with the carbon surface, often referred to as adsorption [23]. Likewise, a higher initial concentration usually results in a greater amount of dye adsorbed [7].

The pseudo-first-order, pseudo-second-order and intraparticle diffusion models were used to analyze the rate of MB adsorption and the results are summarized in *Table 3*. The rate of MB removal corresponds well to the pseudo-second-order model with $R^2 \rightarrow 1$. Therefore, the rate of adsorption is likely controlled by chemisorption, involving the sharing and exchange of electrons between the dye molecules and the functional groups [24],[25]. Further analysis was performed by plotting q_t vs. $t^{0.5}$ that yielded a linear plot passing through the origin, implying that intraparticle diffusion is the only limiting step [26]. In this work, all the plots are linear with an intercept of $C > 0$, confirming the involvement of intraparticle diffusion, but not as a sole limiting step controlling the adsorption process, except for AC2 at C_o = 5.0 mg/L.

From *Table 3*, AC3 exhibits a higher rate constant, k_2, compared to AC1, indicating a steeper gradient before equilibrium is reached over a short period of time. The swift initial adsorption phase can be attributed to its greater specific area that facilitates the rapid diffusion of methylene blue molecules onto its surface. Moreover, the large pore volume allows more accessible pathways to interact with the carbon surface [7],[23]. When an adsorbent has a high affinity for a specific adsorbate, the interactions between them are strong enough to facilitate rapid adsorption. As a result, AC3 could effectively capture MB molecules, making it particularly suitable for applications that require the immediate removal of contaminants.

3.4. Adsorption thermodynamics

At higher temperatures, the reduction in viscosity allows the dye molecules to move more freely in the solution [27], thereby facilitating rapid diffusion across the external boundary layer and into the internal pores of the activated carbon, increasing the overall adsorption capacity of the system [28]. The increase in the temperature of the solution also causes thermal vibration that helps to overcome weak intermolecular forces that hold the aggregates (clustered dye molecules) together [29],[30].

The concept of Gibbs free energy ($\Delta G° = \Delta H° - T\Delta S°$) is crucial to understand the thermodynamics of the adsorption process. To determine the enthalpy, $\Delta H°$, and entropy, $\Delta S°$, the graph of ln K vs. $1/T$ was plotted as

Table 3: The constants of kinetic models for methylene blue adsorption by KOH-activated carbons

C_o (mg/L)		5.0			8.5			14.5			25.0	
Sample	AC1	AC2	AC3	AC1	AC2	AC3	AC1	AC2	AC3	AC1	AC2	AC3
Pseudo-first-order												
q_e (mg/g)	6.59	4.85	4.90	7.77	6.59	6.50	13.1	8.68	7.16	19.3	8.11	9.71
k_1 (min^{-1})	0.0039	0.0026	0.0089	0.0062	0.0100	0.0063	0.0042	0.0051	0.0057	0.0035	0.0048	0.0063
SSE	3.96	1.79	6.68	1.25	16.6	4.19	7.16	5.46	3.16	8.59	2.94	7.28
R^2	0.956	0.965	0.877	0.993	0.935	0.970	0.986	0.975	0.977	0.991	0.982	0.969
Pseudo-second-order												
q_e (mg/g)	7.75	6.11	5.51	8.55	6.94	7.08	14.7	9.52	7.84	22.4	9.01	10.5
k_2 (g/mg min)	0.0006	0.0004	0.0022	0.0010	0.0011	0.0013	0.0004	0.0008	0.0010	0.0002	0.0007	0.0009
SSE	2.32	1.55	3.03	0.370	0.810	0.786	1.75	1.28	0.816	3.29	1.18	2.08
R^2	0.974	0.973	0.935	0.998	0.993	0.993	0.996	0.993	0.993	0.997	0.993	0.990
Intraparticle diffusion												
K_p (mg/g $min^{½}$)	0.196	0.135	0.135	0.168	0.142	0.137	0.309	0.196	0.160	0.485	0.194	0.219
C	0.246	0.00	1.18	1.71	1.09	1.58	1.48	1.47	1.32	0.823	0.921	1.79
SSE	7.40	3.29	4.20	28.4	15.1	12.7	34.5	18.3	17.1	45.7	16.0	28.6
R^2	0.916	0.944	0.901	0.805	0.848	0.860	0.917	0.893	0.859	0.952	0.900	0.865

shown in *Figure 7*. The thermodynamic parameters for MB adsorption by AC1 are summarized in *Table 4*. A positive $\Delta H°$ indicates that the adsorption process is endothermic, with increasing MB removal as the temperature of the solution rises, suggesting that more energy is required to increase the level of adsorption. A high $\Delta H°$ (> 80 kJ/mol) typically indicates that adsorption involves the formation of strong chemical bonds such as covalent or ionic bonds. Accordingly, breaking these bonds requires a substantial amount of energy [31]. The positive $\Delta S°$ suggests an increase in the disorder or randomness of the adsorption system. As dye molecules approach the carbon surface, they lose some of their translational and rotational freedom but might gain additional degrees of freedom due to interactions at the interface, leading to an overall increase in entropy.

The formation of new bonds during chemisorption can create more complex structures, which may facilitate an increase in molecular motion or rearrangement, contributing to a positive entropy change. On the other hand, $\Delta G°$ describes the spontaneity and feasibility of adsorption [14]. The negative $\Delta G°$ proves that the process is thermodynamically favorable.

3.5. Regeneration of activated carbon

The regeneration of activated carbon, which is essential to restore its effectiveness, involves several cycles of adsorption and desorption. In this work, spent AC1 was regenerated using 0.1 M HC1 and distilled water. The efficiency of adsorption and desorption after four cycles is shown in *Figure 8*. Clearly, adsorption and desorption decreased as the number of cycles increased. Both solvents become less effective at restoring the adsorptive characteristics of AC1 over the successive cycles. The desorption capacity remains small throughout all cycles. Notably, the desorption capacity falls closely in line with the subsequent adsorption capacity, a feature of chemisorption [24],[25]. Once adsorbed, it may not be easy for these molecules to desorb without a substantial energy input or chemical alteration.

The desorption efficiency of HCl peaks in cycle 3 (83.0 %) but declines to 63.3 % in cycle 4, suggesting that the solvent becomes less efficient over time. Likewise, the desorption efficiency of water is 166 % in cycle 3 but sharply declines to 36.8 % in cycle 4. Overall, the use of HCl appears to be more consistent over several cycles, even though its efficiency and adsorption capacity gradually decline. Analyzing the global trend

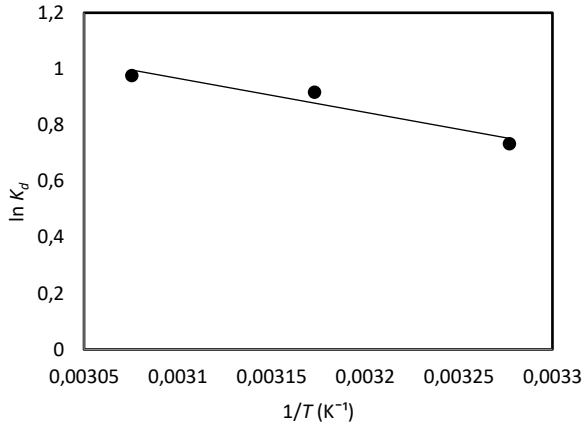

Figure 7: The van't Hoff plot for methylene blue adsorption by AC1

Table 4: Thermodynamic parameters for methylene blue adsorption by AC1

C_o (mg/L)	K_d	T (K)	$\Delta G°$ (kJ.mol)	$\Delta H°$ (kJ/mol)	$\Delta S°$ (kJ/mol.K)
57.4	2.08	305	-1.91	10.1	0.04
50.9	2.50	315	-2.30		
58.4	2.65	325	-2.69		

for both solvents, HCl would be a better option to stabilize carbon regeneration. The performance of HCl could be attributed to the dissolution and displacement of MB molecules on the active sites due to electrostatic repulsion [33],[34].

4. Conclusions

Samples of activated carbon were prepared from palm kernel shell using fresh KOH activator and recycled KOH. The activated carbon produced using the second recycled KOH solution (AC3) exhibits a higher specific surface area of 55.1 m²/g when compared to one prepared using fresh KOH solution (AC1, 7.24 m²/g). Accordingly, the former removes more methylene blue, highlighting the feasibility of using recycled activator solution for the subsequent preparation of activated carbon. Nonetheless, AC1 still demonstrates a strong affinity for methylene blue due to its plentiful supply of surface functional groups. The fitting of adsorption models suggests that adsorption is driven by physicochemical interactions. The thermodynamic parameters conclude that the process is endothermic and spontaneous at high solution temperatures, thereby supporting the viability of using activated carbon for wastewater treatment applications. The regeneration by 0.1 M HCl is more consistent and effective over multiple adsorption-desorption runs and long-term use.

Acknowledgement

This work was funded by UTM Fundamental Research Grant No. 23H09.

(a)

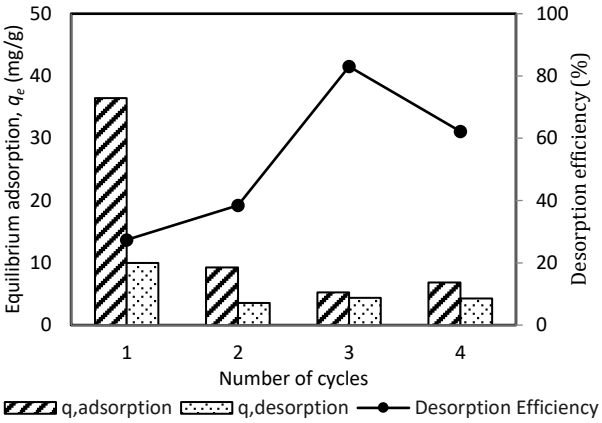

(b)

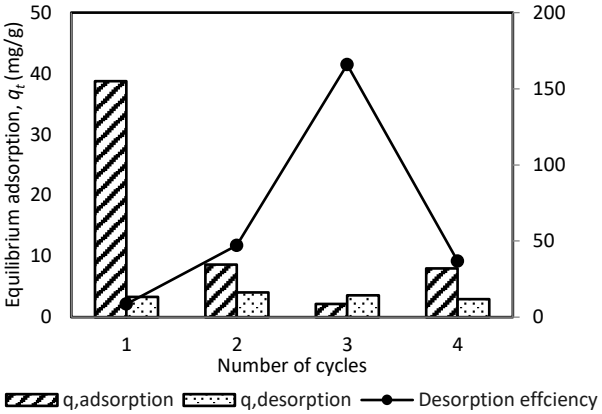

Figure 8: The efficiencies of adsorption and desorption after regeneration using (a) 0.1 M HCl and (b) distilled water

REFERENCES

[1] Xu, R.; Chi, T.; Tian, J.; Chen, L.: A new sustainable wastewater management: Simultaneous mineralization and dehalogenation treatment of high salinity dye wastewater, *J. Clean. Prod.*, 2024, **445**, 141046, DOI: 10.1016/j.jclepro.2024.141046

[2] Prasetyo, H.; Norrdin, M.N.A.M.; Othman, M.H.D.; Jaafar, J.; Yoshioka, T.; Li, Z.; Rahman, M.A.: Technologies for treating wastewater from textile industry: A review, *Mater. Today Proc.*, 2022, **65**, 3066–3072, DOI: 10.1016/j.matpr.2022.04.214

[3] Ming-Twang, S.; Zaini, M.A.A.; Salleh, L.M.; Yunus, M.A.C.; Naushad, M.: Potassium hydroxide-treated palm kernel shell sorbents for the efficient removal of methyl violet dye, *Desalin. Water Treat.*, 2017, **84**, 262–270, DOI: 10.5004/dwt.2017.21206

[4] Zaini, M.A.A.; Meng, T.W.; Kamaruddin, M.J.; Setapar, S.H.M.; Yunus, M.A.C.: Microwave-induced zinc chloride activated palm kernel shell for dye removal, *Sains Malays.*, 2014, **43**(9), 1421–1428

[5] Li, W.; Zhang, D.; Yan, Y.; Dai, Y.; Al-Shiaani, N.H.A.; Zhao, S.; Chen, K.; Guo, A.; Liu, H.; Liu, D.: Ultrasound-assisted successive recovery of chemical activation agent and synthesis of high sulfur petroleum coke-based carbon anode with progressively improving performance K-ion storage, *Appl. Energy*, 2023, **348**, 121567, DOI: 10.1016/j.apenergy.2023.121567

[6] Daneshvar, E.; Vazirzadeh, A.; Niazi, A.; Kousha, M.; Naushad, M.; Bhatnagar, A.: Desorption of methylene blue dye from brown macroalga: Effects of operating parameters, isotherm study and kinetic modelling, *J. Clean. Prod.*, 2017, **152**, 443–453, DOI: 10.1016/j.jclepro.2017.03.119

[7] Kamalanathan, S.; Amran, F.; Zaini, M.A.A.: Oxidized mangosteen peel-derived hydrochar for the removal of methylene blue, *Hung. J. Ind. Chem.*, 2025, **53**(1), 1–7, DOI: 10.33927/hjic-2025-01
[8] Naushad, M.; Khan, M.R.; ALOthman, Z.A.; Al-Muhtaseb, A.H.; Awual, M.R.; Alqadami, A.A.: Water purification using cost effective material prepared from agricultural waste: Kinetics, isotherms, and thermodynamic studies, *CLEAN - Soil Air Water*, 2016, **44**(8), 1036–1045, DOI: 10.1002/clen.201600027
[9] Lozano-Castelló, D.; Calo, J.M.; Cazorla-Amorós, D.; Linares-Solano, A.: Carbon activation with KOH as explored by temperature programmed techniques, and the effects of hydrogen, *Carbon*, 2007, **45**(13), 2529–2536, DOI: 10.1016/j.carbon.2007.08.021
[10] Yang, H.M.; Zhang, D.H.; Chen, Y.; Ran, M.J.; Gu, J.C.: Study on the application of KOH to produce activated carbon to realize the utilization of distiller's grains, *IOP Conf. Ser.: Earth Environ. Sci.*, 2017, **69**, 012051, DOI: 10.1088/1755-1315/69/1/012051
[11] Wang, J.; Ma, J.; Sun, Y.: Adsorption of methylene blue by coal-based activated carbon in high-salt wastewater, *Water*, 2022, **14**(21), 3576, DOI: 10.3390/w14213576
[12] Mousavi, S.A.; Shahbazi, D.; Mahmoudi, A.; Darvishi, P.: Methylene blue removal using prepared activated carbon from grape wood wastes: adsorption process analysis and modeling, *Water Qual. Res. J.*, 2022, **57**(1), 1–19, DOI: 10.2166/wqrj.2021.015
[13] Gao, J.-J.; Qin, Y.-B.; Zhou, T.; Cao, D.-D.; Xu, P.; Hochstetter, D.; Wang, Y.-F.: Adsorption of methylene blue onto activated carbon produced from tea (*Camellia sinensis* L.) seed shells: kinetics, equilibrium, and thermodynamics studies, *J. Zhejiang Univ. Sci. B*, 2013, **14**(7), 650–658, DOI: 10.1631/jzus.b12a0225
[14] Usman-Cholik, M.A.; Amran, F.; Zaini, M.A.A: Zinc chloride-activated denim waste carbon for methylene blue removal, *Ovidius Univ. Ann. Chem.*, 2024, **35**, 105–110, DOI: 10.2478/auoc-2024-0014
[15] Sulaiman, N.S; Amini, M.H.M; Danish, M; Sulaiman, O; Hashim, R: Kinetics, thermodynamics, and isotherms of methylene blue adsorption study onto cassava stem activated carbon, *Water*, 2021, **13**(20), 2936, DOI: 10.3390/w13202936
[16] Biswas, S.; Rashid, T.U.; Debnath, T.; Haque, P.; Rahman, M.M.: Application of chitosan-clay biocomposite beads for removal of heavy metal and dye from industrial effluent, *J. Compos. Sci.*, 2020, **4**(1), 16, DOI: 10.3390/jcs4010016
[17] El-Bery, H.M.; Saleh, M.; El-Gendy, R.A.; Saleh, M.R.; Thabet, S.M.: High adsorption capacity of phenol and methylene blue using activated carbon derived from lignocellulosic agriculture wastes, *Sci. Rep.*, 2022, **12**, 5499, DOI: 10.1038/s41598-022-09475-4
[18] Zaini, M.A.A.; Okayama, R.; Machida, M.: Adsorption of aqueous metal ions on cattle-manure-compost based activated carbons, *J. Hazard. Mater.*, 2009, **170**(2-3), 1119–1124, DOI: 10.1016/j.jhazmat.2009.05.090
[19] Oladoye, P.O.; Ajiboye, T.O.; Omotola, E.O.; Oyewola, O.J.: Methylene blue dye: Toxicity and potential elimination technology from wastewater, *Results Eng.*, 2022, **16**, 100678, DOI: 10.1016/j.rineng.2022.100678
[20] Idan, I.J; Abdullah, L.C; Choong, T.S.Y; Jamil, S.N.A.M: Equilibrium, kinetics and thermodynamic adsorption studies of acid dyes on adsorbent developed from kenaf core fiber, *Adsorpt. Sci. Technol.*, 2018, **36**(1-2), 694–712, DOI: 10.1177/0263617417715532
[21] Sultana, M.; Rownok, M.H.; Sabrin, M.; Rahaman, M.H.; Alam, S.M.N.: A review on experimental chemically modified activated carbon to enhance dye and heavy metals adsorption, *Clean. Eng. Technol.*, 2022, **6**, 100382, DOI: 10.1016/j.clet.2021.100382
[22] Kalam, S.; Abu-Khamsin, S.A.; Kamal, M.S.; Patil, S. Surfactant adsorption isotherms: A review, *ACS Omega*, 2021, **6**(48), 32342–32348, DOI: 10.1021/acsomega.1c04661
[23] Hameed, B.H.; Salman, J.M.; Ahmad, A.L.: Adsorption isotherm and kinetic modeling of 2,4-D pesticide on activated carbon derived from date stones, *J. Hazard. Mater.*, 2009, **163**(1), 121–126, DOI: 10.1016/j.jhazmat.2008.06.069
[24] Wolski, R.; Bazan-Wozniak, A.; Pietrzak, R.: Adsorption of methyl red and methylene blue on carbon bioadsorbents obtained from biogas plant waste materials, *Molecules*, 2023, **28**(18), 6712, DOI: 10.3390/molecules28186712
[25] Somsiripan, T.; Sangwichien, C.: Enhancement of adsorption capacity of methylene blue, malachite green, and rhodamine B onto KOH activated carbon derived from oil palm empty fruit bunches, *Arab. J. Chem.*, 2023, **16**(12), 105270, DOI: 10.1016/j.arabjc.2023.105270
[26] Tan, I.A.W.; Ahmad, A.L.; Hameed, B.H.: Adsorption isotherms, kinetics, thermodynamics and desorption studies of 2,4,6-trichlorophenol on oil palm empty fruit bunch-based activated carbon, *J. Hazard. Mater.*, 2009, **164**(2-3), 473–482, DOI: 10.1016/j.jhazmat.2008.08.025
[27] Smoczynski, L.; Pierozynski, B.; Mikolajczyk, T.: The effect of temperature on the biosorption of dyes from aqueous solutions, *Processes*, 2020, **8**(6), 636, DOI: 10.3390/pr8060636
[28] Vysniauskas, A.; Qurashi, M.; Gallop, N.; Balaz, M.; Anderson, H.L.; Kuimova, M.K.: Unravelling the effect of temperature on viscosity-sensitive fluorescent molecular rotors, *Chem. Sci.*, 2015, **6**(10), 5773–5778, DOI: 10.1039/c5sc02248g
[29] Furuyama, T.; Uchiyama, S.; Chikamatsu, T.; Horikawa, T.; Maeda, H.; Segi, M., Takahashi, H.; Taima, T.: Temperature-dependent changes in the molecular orientation and visible color of phthalocyanine films, *RSC Adv.*, 2020, **10**(52), 31348–31354, DOI: 10.1039/d0ra06273a

[30] Kumawat, L.K.; Abogunrin, A.A.; Kickham, M.; Pardeshi, J.; Fenelon, O.; Schroeder, M.; Elmes, R.B.P.: Squaramide-naphthalimide conjugates as “turn-on” fluorescent sensors for bromide through an aggregation-disaggregation approach, *Front. Chem.*, 2019, **7**, 354, DOI: 10.3389/fchem.2019.00354

[31] Ebelegi, A.N.; Ayawei, N.; Wankasi, D.: Interpretation of adsorption thermodynamics and kinetics, *Open J. Phys. Chem.*, 2020, **10**(3), 166–182, DOI: 10.4236/ojpc.2020.103010

[32] Mardare, A.: High throughput growth, modification and characterization of thin anodic oxides on valve metals (PhD thesis), 2009, Ruhr-Universität Bochum, Fakultät für Physik und Astronomie, Bochum, Germany

[33] Vijayaraghavan, K.; Lee, M.W.; Yun, Y.-S.: A new approach to study the decolorization of complex reactive dye bath effluent by biosorption technique, *Biores. Technol.*, 2008, **99**(13), 5778–5785, DOI: 10.1016/j.biortech.2007.10.012

[34] Abdallah, R.; Taha, S.: Biosorption of methylene blue from aqueous solution by nonviable *Aspergillus fumigatus*, *Chem. Eng. J.*, 2012, **195-196**, 69–76, DOI: 10.1016/j.cej.2012.04.066